THE ASTROPHYSICAL JOURNAL, 837:164 (5pp), 2017 March 10 https://doi.org/10.3847/1538-4357/aa6218

A Simple Analytical Model for Rocky Planet Interiors

Li Zeng, (曾理) and Stein B. Jacobsen
Department of Earth and Planetary Sciences, Harvard University, Cambridge, MA 02138, USA; astrozeng@gmail.com, jacobsen@neodymium.harvard.edu
Received 2016 June 10; revised 2016 August 2; accepted 2016 August 2; published 2017 March 15

Abstract

This work aims to explore the scaling relations among rocky exoplanets. The assumption that the internal gravity increases linearly in the core and stays constant in the mantle is tested against numerical simulations, and a simple model is constructed, applicable to rocky exoplanets of CMF (core mass fraction) = 0.2–0.35 and mass = 0.1–30 $M_\oplus$. Various scaling relations are derived: (1) CMF $\approx$ CRF^2 (core radius fraction squared), (2) $P_{\rm typical} \sim g_s^2$ (typical interior pressure scales as surface gravity squared), (3) energy released in core formation is $\sim\frac{1}{10}$ the total gravitational energy, (4) effective heat capacity of the mantle $\approx\left(\frac{M_p}{M_\oplus}\right) \times 7.5 \times 10^{27}$ J K^{-1}, (5) moment of inertia $\approx\frac{1}{3}M_p R_p^2$. These relations, though approximate, are handy for quick use owing to their simplicity and lucidity, and provide insights into the interior structures of those exoplanets.

Key words: Earth – planets and satellites: composition – planets and satellites: fundamental parameters – planets and satellites: interiors – planets and satellites: terrestrial planets

1. Introduction

Since the masses and radii of about a dozen rocky exoplanets have been found and more are likely, we explore what other parameters can also be gleaned from this information. Our earlier work (Zeng et al. 2016) shows that by using an equation of state (EOS) for Earth, a simple relationship between the core mass fraction (CMF), planetary radius, and mass for different CMFs can be found as

$$\mathrm{CMF} = \frac{1}{0.21}\left[1.07 - \left(\frac{R}{R_\oplus}\right)\Big/\left(\frac{M}{M_\oplus}\right)^{0.27}\right]. \quad (1)$$

This work shows that the CMF can be related to the CRF (core radius fraction) of a rocky planet. A simple structural model can be devised that depends only on three parameters: (1) surface gravity g_s, (2) planet radius R_p, and (3) CRF. The procedure is as follows:

1. Surface gravity $g_s = \frac{GM_p}{R_p^2}$ can be calculated from the mass M_p and radius R_p of a rocky planet, or directly by combining the depth of transit with the amplitude of radial velocity (Equation (16)).
2. CMF can be determined from Equation (1).
3. CRF can be estimated as $\sqrt{\mathrm{CMF}}$.

The sole assumption of this model is that the internal gravity profile of the planet can be approximated as a piecewise function (see Figure 1):

1. In the core, the gravity g increases linearly with radius from 0 at the center to g_s (surface value) at the CMB (core–mantle boundary): $g_{\rm core}(r) = g_s\left(\frac{r}{R_{\rm core}}\right) \propto r$
2. In the mantle, g stays constant: $g_{\rm mantle}(r) = g_s = $ const.

This assumption is equivalent to assuming a constant core density, followed by the density decreasing to two-thirds of the core density at the CMB, and the density deceasing as $1/r$ in the mantle.

The validity of this assumption is tested against the numerical results from solving the planetary structures with a realistic EOS derived from the Preliminary Reference Earth Model (PREM; Dziewonski & Anderson 1981), across the mass–radius range 0.1–30 $M_\oplus$ and $0.2 \lesssim \mathrm{CMF} \lesssim 0.35$ for two-layer (core+mantle) rocky planets. Note that Mercury lies outside this range of CMF because it has a big core, owing to its likely origin in a giant impact (Asphaug & Reufer 2014).

Various scaling relations can be derived from this model.

2. Scaling Relation between Pressure and Gravity

The two first-order differential equations (Seager et al. 2007; Zeng & Seager 2008; Zeng & Sasselov 2013) governing rocky planet interiors are:

(1) hydrostatic equilibrium (force balance) equation:

$$\frac{dP}{dr} = -\frac{Gm\rho}{r^2} = -g\rho \quad (2)$$

(2) mass conservation equation:

$$\frac{dm}{dr} = 4\pi r^2 \rho. \quad (3)$$

Equations (2) and (3) can be combined to give a relation between the internal pressure P and the mass m (mass contained within radius r, now used as the independent variable instead):

$$\frac{dP}{dm} = -\frac{Gm}{4\pi r^4} = -\frac{1}{4\pi G}\frac{g^2}{m} = -\frac{1}{4\pi G}g^2\frac{d\ln(m)}{dm}. \quad (4)$$

Integrating Equation (4), we get ($\ln(m)$ stands for natural logarithmic of m)

$$\int_{\rm surface}^{\rm interior} dP = -\frac{1}{4\pi G}\int_{M_p}^{\text{mass enclosed inside}} g^2 d\ln(m). \quad (5)$$

This integration is from the surface inward, because the pressure at the surface is zero. Therefore, the typical internal

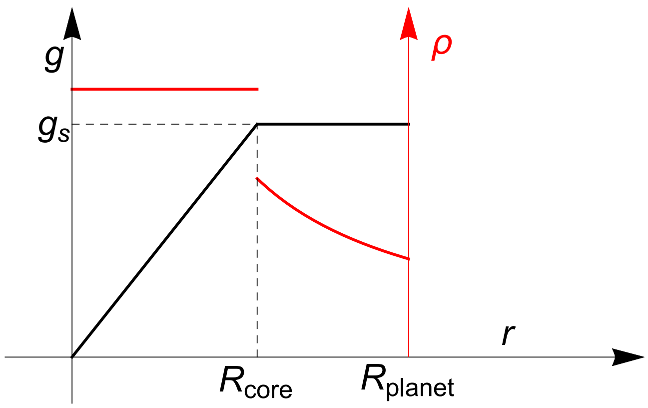

Figure 1. Profiles of the gravity (black) and density (red) of the approximation.

pressure is of the order of

$$P \sim \frac{\overline{g^2}}{4\pi G} \tag{6}$$

where $\overline{g^2}$ is an average of g^2. The mean density of the planet is defined as $\overline{\rho_p}$. The surface gravity g_s and characteristic interior pressure P_{typical} are

$$g_s \equiv \frac{GM_p}{R_p^2} \tag{7}$$

$$P_{\text{typical}} \equiv \frac{{g_s}^2}{4\pi G} = \frac{GM_p^2}{4\pi R_p^4}. \tag{8}$$

Later on, P_{typical} is shown to approximate P_{CMB} (the pressure at the CMB). If g_s is given in S.I. units (m s^{-2}) and P_{typical} in GPa, then

$$P_{\text{typical}} \sim g_s^2. \tag{9}$$

For example, $g_\oplus$ (Earth's gravity) ≈ 10 m s^{-2}, $g_\oplus^2 \approx 100$ GPa is near $P_{\oplus,\text{CMB}} = 136$ GPa.

3. Density Profile

Based on the assumption of the gravity profile, the density profile is

$$\rho_{\text{core}}(r) = \frac{3g_s}{4\pi G R_{\text{core}}} = \overline{\rho_p}\,\frac{1}{\text{CRF}} = \text{constant, and } m_{\text{core}}(r) \propto r^3 \tag{10a}$$

$$\rho_{\text{mantle}}(r) = \frac{g_s}{2\pi G r} \propto \frac{1}{r}, \text{ and } m_{\text{mantle}}(r) \propto r^2. \tag{10b}$$

Figure 2 compares it to the PREM density profile (Dziewonski & Anderson 1981). Notice that g is always continuous in r, but ρ may have discontinuities. The $1/r$ dependence approximates the compression of mantle material with increasing depth, and the relatively small core (CMF $\lesssim 0.35$) allows the core density to be approximated as constant. Anywhere in the mantle,

$$\frac{m}{M_p} = \left(\frac{r}{R_p}\right)^2. \tag{11}$$

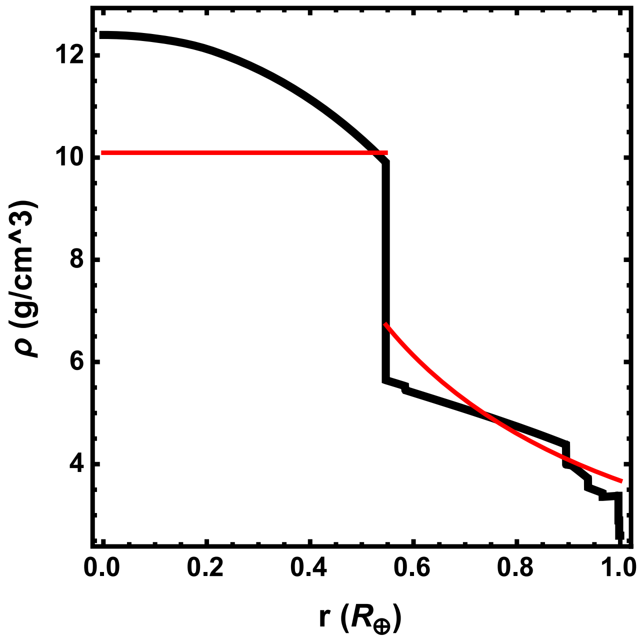

Figure 2. Black: PREM density profile. Red: approximation.

In particular, at the CMB,

$$\text{CMF} = \frac{M_{\text{core}}}{M_p} = \left(\frac{R_{\text{core}}}{R_p}\right)^2 = \text{CRF}^2. \tag{12}$$

In reality, this exact relation becomes approximate:

$$\text{CMF} \approx \text{CRF}^2 \text{ or } \text{CRF} \approx \sqrt{\text{CMF}}. \tag{13}$$

For example, applying Equation (13) to Earth and Kepler-93b (Ballard et al. 2014; Dressing et al. 2015) gives

1. For Earth, $\text{CMF}_\oplus = 0.325$ and $\text{CRF}_\oplus = \frac{3480\text{ km}}{6371\text{ km}} = 0.546$. So $\text{CRF}_\oplus^2 = 0.546^2 = 0.298$, which is $\sim 9\%$ smaller than 0.325.
2. For Kepler-93b, numerical calculations in Zeng et al. (2016) give $\text{CMF}_{\text{K93b}} = 0.278$ and $\text{CRF}_{\text{K93b}} = 0.493$. So $\text{CRF}_{\text{K93b}}^2 = 0.243$, which is $\sim 12\%$ smaller than 0.278.

In reality, CRF^2 tends to underestimate the CMF by $\sim 10\%$. Nevertheless, it is a quick method to estimate the CMF from the CRF and vice versa.

Earth-like rocky planets have CMF ~ 0.3 and CRF ~ 0.5. Equation (13) can even be generalized to a rocky planet with a volatile envelope when it is applied only to the solid portion of that planet.

4. Pressure Profile

4.1. Pressure in the Mantle

Integrating Equation (5) with constant mantle gravity gives

$$P_{\text{mantle}}(m) = \frac{g_s^2}{4\pi G} \ln\left(\frac{M_p}{m}\right) = P_{\text{typical}} \ln\left(\frac{M_p}{m}\right) = 2P_{\text{typical}} \ln\left(\frac{R_p}{r}\right) \tag{14}$$

Equation (14) gives $P_{\rm CMB}$:

$$P_{\rm CMB} = P_{\rm typical} \ln\left(\frac{1}{\rm CMF}\right) = \frac{g_s^2}{4\pi G}\left(\frac{1}{\rm CMF}\right). \tag{15}$$

For CMF = 0.2–0.35, $P_{\rm CMB} = (1.0\text{–}1.6)P_{\rm typical}$.

$P_{\rm CMB}$ is an important physical parameter, because it determines the state of core and mantle materials in contact. g_s can be determined independently of the stellar parameters (Southworth et al. 2007) as

$$g_s = \frac{2\pi}{P_{\rm orb}} \frac{(1-e^2)^{1/2} A_{RV}}{(R/a)^2 \sin(i)} \tag{16}$$

where the semi-amplitude A_{RV} and orbital eccentricity e can be constrained from the radial-velocity curve, and R/a is the ratio of radius to semimajor axis, which could be constrained directly from the transit light curve. The orbital period $P_{\rm orb}$ can be constrained from both. Thus, it is possible to estimate $P_{\rm CMB}$ even without knowing the mass and radius accurately in some cases for rocky planets.

4.2. Range of Applicability of This Model

From a theoretical point, we explore the range of applicability of this model.

The bulk modulus is $K \equiv \frac{\partial P}{\partial \ln(\rho)}$. Therefore, in the mantle

$$K_{\rm mantle} = \frac{\partial P_{\rm mantle}}{\partial \ln(\rho_{\rm mantle})} = \frac{g_s^2}{4\pi G}\frac{d\ln(m)}{d\ln(r)} = 2P_{\rm typical}. \tag{17}$$

Thus, in the model, the bulk modulus is constant everywhere in the mantle and equal to twice the typical internal pressure $P_{\rm typical}$. Realistically, K will increase with pressure, so how good is this approximation?

For Earth, $P_{\oplus,\rm typical} = \frac{g_\oplus^2}{4\pi G} = 115$ GPa, so $K_{\oplus,\rm mantle} = 230$ GPa. Comparing it to the isentropic bulk modulus K_s of Earth's mantle according to PREM, we have $K_{\oplus,\rm LID} = 130$ GPa, $K_{\oplus,670\ \rm km}$ 255.6–300 GPa, and $K_{\oplus,\rm D''} = 640$ GPa.

So $K_{\oplus,\rm mantle}$ represents the middle of the range for the realistic bulk modulus in the mantle. For higher masses, let us invoke the BM2 (Birch–Murnaghan second-order) EOS (Birch 1947, 1952), which when fitted to PREM gives $K_0 \approx 200$ GPa for both core and mantle (Zeng et al. 2016):

$$P = \frac{3}{2}K_0\left[\left(\frac{\rho}{\rho_0}\right)^{\frac{7}{3}} - \left(\frac{\rho}{\rho_0}\right)^{\frac{5}{3}}\right]. \tag{18}$$

Again, K is obtained by differentiating Equation (18):

$$K \equiv \frac{\partial P}{\partial \ln(\rho/\rho_0)} = \frac{3}{2}K_0\left[\frac{7}{3}\left(\frac{\rho}{\rho_0}\right)^{\frac{7}{3}} - \frac{5}{3}\left(\frac{\rho}{\rho_0}\right)^{\frac{5}{3}}\right]. \tag{19}$$

Equation (19) suggests that $K \approx K_0$ when $P \lesssim K_0$ and $K \to \frac{7}{3}P \approx 2P$ when $P \gg K_0$. Since $P_{\rm typical}$ is the typical pressure in the mantle, $K \approx 2P \approx 2P_{\rm typical}$. This is the same as Equation (17). Therefore, this approximation will hold for higher masses as long as the BM2 EOS holds. The BM2 EOS fails around 30 $M_\oplus$, so the range of validity of this model extends up to 30 $M_\oplus$.

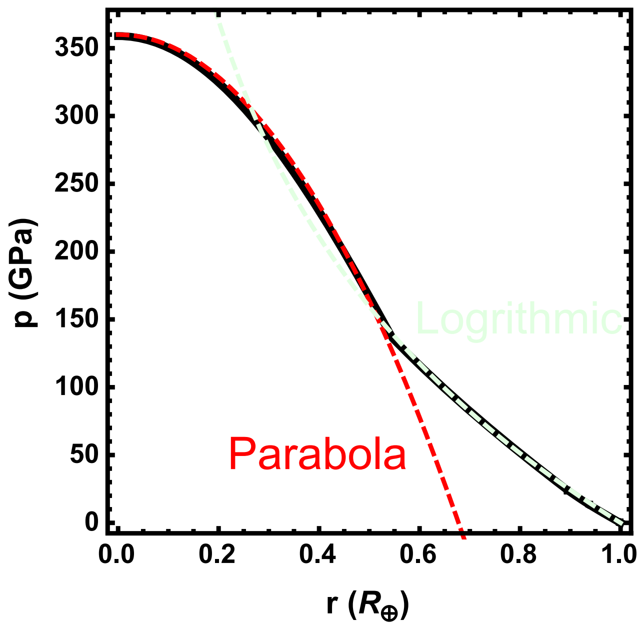

Figure 3. Piecewise approximation to the pressure profile inside Earth (generally applicable to two-layer rocky planets with $0.2 \lesssim$ CMF $\lesssim 0.35$). Black curve: pressure profile from PREM. Red dashed curve: parabolic function in radius as an approximation for pressure in the core. Light-green dashed curve: logarithmic function in radius as an approximation for pressure in the mantle.

4.3. Pressure in the Core

Since $\rho_{\rm core}$ = const. in this approximation, from Equation (2) we have

$$\frac{dP_{\rm core}(r)}{dr} = -\frac{G}{r^2}\left(\frac{g_s}{GR_{\rm core}}r^3\right)\left(\frac{3g_s}{4\pi GR_{\rm core}}\right) = -\frac{3r}{R_{\rm core}^2}P_{\rm typical}. \tag{20}$$

Integrating it gives the dependence of pressure on radius as a parabolic function:

$$P_{\rm core}(r) = P_0 - \frac{3}{2}P_{\rm typical}\left(\frac{r}{R_{\rm core}}\right)^2 \tag{21}$$

P_0 (central pressure) can be determined by connecting it to $P_{\rm CMB}$ at the CMB as

$$P_0 = P_{\rm CMB} + \frac{3}{2}P_{\rm typical} = P_{\rm typical}\left[\ln\left(\frac{1}{\rm CMF}\right) + \frac{3}{2}\right] \Rightarrow P_0 \sim 3P_{\rm typical}. \tag{22}$$

Therefore, in this approximation, the dependence of pressure on radius is piecewise: parabolic in the core (Equation (21)), logarithmic in the mantle (Equation (14)), and they interconnect at the CMB. For Earth, this approximate piecewise pressure profile can be closely matched to the realistic pressure profile calculated from PREM as shown in Figure 3.

5. Energy of Core Formation

The energy of core formation can be estimated as the difference in gravitational energies between the uniform-density state and the model. According to the virial theorem

(Haswell 2010), the total gravitational energy is

$$E_{\rm grav} = -3\int_{\rm center}^{\rm surface} \frac{P}{\rho} dm. \tag{23}$$

With the analytic forms of P and ρ in our approximation, Equation (23) can be integrated to give

$$E_{\rm grav} = -\frac{GM_p^2}{3R_p}\left(2 - \frac{1}{5}{\rm CRF}^3\right). \tag{24}$$

Comparing this to the gravitational energy of a uniform-density sphere: $E_{\rm grav,uniform\ sphere} = -\frac{3}{5}\frac{GM_p^2}{R_p}$, the difference of the two can be taken as the energy released during core formation (release of gravitational energy due to concentration of denser materials toward the center):

$$E_{\rm diff} = E_{\rm grav,uniform\ sphere} - E_{\rm grav} = \frac{GM_p^2}{R_p}\left(\frac{1}{15}(1 - {\rm CRF}^3)\right) = \frac{GM_p^2}{R_p}\left(\frac{1}{15}(1 - {\rm CMF}^{3/2})\right). \tag{25}$$

Since $0.2 \lesssim {\rm CMF} \lesssim 0.35$, the term ${\rm CMF}^{3/2}$ is small enough to be dropped, which gives

$$E_{\rm diff} \approx \frac{1}{15}\frac{GM_p^2}{R_p} \approx \frac{1}{10}|E_{\rm grav}|. \tag{26}$$

Therefore, the energy released during core formation is ~10% of the total gravitational energy of such an Earth-like rocky planet. For Earth, $E_{\rm diff,\oplus} \approx 2.5 \times 10^{31}$ J.

6. Thermal Content of the Planet

Since the temperatures inside the mantle of such a planet are likely above the Debye temperature of the solid, the heat capacity per mole of atoms can be approximated as $3R$ (gas constant $R = 8.314\ {\rm J\ K^{-1}\ mol^{-1}}$). The specific heat capacity (heat capacity per unit mass) is $3R/\mu$ where μ is the average atomic weight of the composition, which for Mg silicates (MgO, SiO_2, or their combination in any proportion, such as $MgSiO_3$ or Mg_2SiO_4) is $0.02\ {\rm kg\ mol^{-1}}$. The specific thermal energy $u_{\rm th}$ of the mantle material is thus

$$u_{\rm th} = \frac{3RT}{\mu} \tag{27}$$

where T is temperature. The total thermal energy of the mantle is calculated by integration:

$$E_{\rm th,mantle} = \int_{M_{\rm core}}^{M_p} u_{\rm th}\, dm = M_p \int_{\rm CMF}^{1} u_{\rm th}\, dx \tag{28}$$

where $x \equiv \frac{m}{M_p}$. In this model, mantle density $\rho_{\rm mantle} \propto \frac{1}{r} \propto \frac{1}{\sqrt{m}}$ (Equation 10(b)). On the other hand, with the assumption of an adiabatic temperature gradient in the mantle and the introduction of the Grüneisen parameter $\gamma \equiv \frac{\partial \ln(T)}{\partial \ln(\rho)}|_{\rm adiabat}$, the specific thermal energy can be rewritten to show its functional dependence on density ρ or mass m:

$$u_{\rm th} = \frac{3RT_{\rm mp}}{\mu}\left(\frac{\rho}{\rho_0}\right)^{\gamma} = \frac{3RT_{\rm mp}}{\mu}\left(\frac{m}{M_p}\right)^{-\frac{\gamma}{2}} \tag{29}$$

where $T_{\rm mp}$ (mantle potential temperature) is defined as the temperature where the mantle adiabat is extrapolated to zero pressure. $\gamma = 1$ is taken for simplicity. Then,

$$E_{\rm th,mantle} = 2M_p\frac{3RT_{\rm mp}}{\mu}(1 - \sqrt{\rm CMF}) \tag{30}$$

where ${\rm CMF} \approx 0.3$ for the planets concerned, so $\sqrt{\rm CMF} \approx {\rm CRF} \approx 0.5 = \frac{1}{2}$, and the total thermal energy of the mantle (considering only vibrations of atoms in crystal lattices and neglecting the electron contribution) is

$$E_{\rm th,mantle} \downarrow\approx \frac{3RT_{\rm mp}}{\mu}M_p \downarrow\approx \left(\frac{T_{\rm mp}}{1000\ {\rm K}}\right)\left(\frac{M_p}{M_\oplus}\right) \times 7.5 \times 10^{30}\ {\rm J}. \tag{31}$$

An effective heat capacity $C_{\rm th,mantle}$ of the mantle can be defined with respect to $T_{\rm mp}$:

$$C_{\rm th,mantle} \approx \frac{3R}{\mu}M_p \approx \left(\frac{M_p}{M_\oplus}\right) \times 7.5 \times 10^{27}\ {\rm J\ K^{-1}}. \tag{32}$$

Equation (31) suggests that the thermal energy can be calculated by treating the mantle of mass M_p as uncompressed isothermal at $T_{\rm mp}$. For Earth, $T_{\rm mp} \approx 1700$ K, $M_p = 6 \times 10^{24}$ kg, and $\mu = 0.02\ {\rm kg\ mol^{-1}}$ (Stacey & Davis 2008), thus $E_{\rm th,mantle,\oplus} \approx 1.3 \times 10^{31}$ J and $C_{\rm th,mantle,\oplus} \approx 7.5 \times 10^{27}\ {\rm J\ K^{-1}}$.

Detailed calculation in Stacey & Davis (2008) shows that the effective heat capacity of Earth's mantle is $7.4 \times 10^{27}\ {\rm J\ K^{-1}}$, which is very close to our estimate. Since the core is small in comparison and the mantle dictates the cooling of the core (Stacey & Davis 2008), this heat capacity can be regarded as an approximation for the heat capacity of the entire planet, and can generally be applied to rocky exoplanets with estimates of their masses and mantle potential temperatures.

7. Moment of Inertia

The moment of inertia is calculated from the following formula, where x represents the distance of the mass element from the rotational axis:

$$I = \iiint_V \rho(\boldsymbol{r})x^2 dV \tag{33}$$

Consider two simple cases: (i) for a thin spherical shell with radius R_p, $I_{\rm shell} = \frac{2}{3}MR_p^2$; (ii) for a uniform solid sphere with radius R_p, $I_{\rm solid\ sphere} = \frac{2}{5}MR_p^2$.

If $C \equiv I/MR_p^2$ is defined as the moment of inertia factor, then $C = \frac{2}{3}$for a shell and $C = \frac{2}{5}$ for a sphere. Smaller C corresponds to mass being more concentrated toward the center. For this model, the moments of inertia of the core and mantle can each be calculated separately, then combined to give the total moment of inertia of the planet:

$$I_{\rm core} = \frac{2}{5}M_pR_p^2 \times {\rm CMF}^2 \tag{34}$$

$$I_{\rm mantle} = \frac{1}{3}M_pR_p^2 \cdot (1 - {\rm CMF}^2) \tag{35}$$

$$I_{\text{total}} = I_{\text{core}} + I_{\text{mantle}} = \frac{1}{3}M_p R_p^2 \left(1 + \frac{1}{5}\text{CMF}^2\right). \quad (36)$$

Considering that $0.2 \lesssim \text{CMF} \lesssim 0.35$, the term $\frac{1}{5}\text{CMF}^2$ can be ignored, so $C \approx \frac{1}{3}$. In the solar system, the values of C for Mercury, Venus, and Earth are indeed very close to $\frac{1}{3}$ (Rubie et al. 2007). Here $C \approx \frac{1}{3}$ can be generalized to other Earth-like rocky exoplanets:

$$I_{\text{planet}} \approx \frac{1}{3}M_p R_p^2. \quad (37)$$

For Earth, $M_{\oplus} R_{\oplus}^2 = 2.4 \times 10^{38}$ kg m^2 and $I_{\oplus} \approx \frac{1}{3}M_{\oplus} R_{\oplus}^2 = 8 \times 10^{37}$ kg m^2. The angular momentum of Earth's rotation is $L_{\oplus} = I_{\oplus}\Omega_{\oplus} = 6 \times 10^{33}$ kg m^2 s^{-1}. The total rotational energy of Earth is $E_{\text{rot}} = \frac{1}{2}I_{\oplus}\Omega_{\oplus}^2 = \frac{L_{\oplus}^2}{2\Omega_{\oplus}^2} = 2 \times 10^{29}$ J, where $\Omega_{\oplus} = 7.3 \times 10^{-5}$ rad s^{-1} is the angular frequency of Earth's rotation.

8. Conclusion

A simple model for Earth-like rocky planetary interiors is presented here. It predicts that: (1) $\text{CMF} \approx \text{CRF}^2$ or $\text{CRF} \approx \sqrt{\text{CMF}}$ (a relation exists between the core mass fraction and the core radius fraction of a planet), (2) $P_{\text{typical}} \sim g_s^2$ (the typical interior pressure scales as the surface gravity squared), (3) $E_{\text{diff}} \approx \frac{1}{10}|E_{\text{grav}}|$ (the energy released in core formation is about a tenth of the total gravitational energy), (4) the effective heat capacity of the mantle $C_{\text{th,mantle}} \approx \left(\frac{M_p}{M_{\oplus}}\right) \times 7.5 \times 10^{27}$ J K^{-1}, and (5) the total moment of inertia of a planet $I_{\text{total}} \approx \frac{1}{3}M_p R_p^2$. More results could be derived from this model as well.

Although they are approximate, these relations are straightforward to apply, because in many cases mass and radius are measured only approximately anyway. Combined with the mass–radius relation (Equation (1)) of Zeng et al. (2016) and Zeng & Jacobsen (2016), these formulae give us some insight and intuition toward understanding rocky planetary interiors, and they complement the exact numerical approach.

This work was supported by a grant from the Simons Foundation (SCOL [award #337090] to L.Z.). The authors would like to thank Mr. and Mrs. Simons and the Simons Foundation for generously supporting this research project. The author Li Zeng would like to thank his father Lingwei Zeng (曾令维) and mother Ling Li (李玲) for continuous support and help. He also would like to thank Eugenia Hyung (刑噶辰) for insightful discussion on this paper. Part of this research was also conducted under the Sandia Z Fundamental Science Program and supported by the Department of Energy National Nuclear Security Administration under Award Numbers DE-NA0001804 and DE-NA0002937 to S. B. Jacobsen (PI) with Harvard University. This research is the authors' views and not those of the DOE. The authors would like to thank Dimitar D. Sasselov for insightful suggestions and helpful comments on this paper.

References

Asphaug, E., & Reufer, A. 2014, NatGe, 7, 564
Ballard, S., Huber, D., Chaplin, W., et al. 2014, ApJ, 790, 12
Birch, F. 1947, PhRv, 71, 809
Birch, F. 1952, JGR, 57, 227
Dressing, C. D., Charbonneau, D., Dumusque, X., et al. 2015, ApJ, 800, 135
Dziewonski, A. M., & Anderson, D. L. 1981, PEPI, 25, 297
Haswell, C. A. 2010, Transiting Exoplanets (Cambridge: Cambridge Univ. Press)
Rubie, D., Nimmo, F., & Melosh, H. 2007, in Treatise on Geophysics, ed. G. Schubert (Amsterdam: Elsevier), 51
Seager, S., Kuchner, M., Hier-Majumder, C. A., & Militzer, B. 2007, ApJ, 669, 1279
Southworth, J., Wheatley, P. J., & Sams, G. 2007, MNRAS, 379, L11
Stacey, F. D., & Davis, P. M. 2008, Physics of the Earth (Cambridge: Cambridge Univ. Press)
Zeng, L., & Jacobsen, S. B. 2016, ApJ, 829, 18
Zeng, L., & Sasselov, D. 2013, PASP, 125, 227
Zeng, L., Sasselov, D. D., & Jacobsen, S. B. 2016, ApJ, 819, 127
Zeng, L., & Seager, S. 2008, PASP, 120, 983